increases to 2.6 W but the efficiency drops to approximately 10 percent. Assuming some RF power loss to the resonant circuit (and lead resistance), these predictions agree reasonably well with the observed performance at 9.6 GHz: 1.8 W, 8.8 percent at $V_B = 18$ V and 2.2 W, 7.1 percent at 28 V.

VIII. Conclusions

It is concluded that Q-mode operation is present in the experimental devices that are supercritically doped for the following reasons. The RF voltage is sufficient for domain quenching or LSA operation, but the LSA mode has been shown not to exist in these devices. All of the experimental characteristics are consistent with the Q mode; for example, power and frequency increase monotonically with bias-voltage increase. The oscillators are widely tunable above the transit time frequency. The chip RF capacitance is two to four times the low-field capacitance. Finally, the RF power and efficiency calculated by Q-mode theory for operation at 20 and 30-V bias are in good agreement with the values measured experimentally, if some RF circuit loss is assumed to be present. Thus experiments with pulse-biased highly doped TE devices have verified Q-mode operation in X-band waveguide circuits over a bias-voltage range from approximately twice to approximately six times the threshold value. A broad frequency range of operation was obtained for proper RF circuit loading of chips in small device packages. The highest efficiency was obtained with GaAs material of n^+-n-n^+ construction which exhibited a current drop of greater than 30 percent.

Analysis of the post-type waveguide circuit showed that oscillation occurs with TE devices when the post to short-plane separation is about one-half waveguide wavelength. When viewed from the chip, the circuit is operating slightly below the frequency of parallel circuit resonance. Circuit RF loading effects were shown to be important for wide bandwidth operation of quenched-domain mode oscillators.

Acknowledgment

The author wishes to thank several companies for providing devices for use in this study: D. Hanson at Hewlett-Packard, L. A. MacKenzie at Monsanto, and T. E. Walsh at RCA.

References

[1] D. D. Khandelwal and W. R. Curtice, "A study of the single-frequency quenched-domain mode Gunn-effect oscillator," *IEEE Trans. Microwave Theory Tech.*, vol. MTT-18, pp. 178–187, Apr. 1970.
[2] H. Pollmann, R. Engelmann, W. Frey, and B. G. Bosch, "Load dependence of Gunn-oscillator performance," *IEEE Trans. Microwave Theory Tech.* (*Special Issue on Microwave Circuit Aspects of Avalanche-Diode and Transferred Electron Devices*), vol. MTT-18, pp. 817–827, Nov. 1970.
[3] T. Ikoma, H. Toritsuka, and H. Yanai, "Observations of current waveforms of the transferred-electron oscillators," in *Proc. 7th Int. Conf. Microwave and Optical Generation and Amplification* (Hamburg, Germany), pp. 401–406, Sept. 1968.
[4] N. Marcuvitz, *Waveguide Handbook.* New York: Dover, 1965, pp. 257–266.
[5] W. C. Tsai, F. J. Rosenbaum, and L. A. MacKenzie, "Circuit analysis of waveguide-cavity Gunn-effect oscillator," *IEEE Trans. Microwave Theory Tech.* (*Special Issue on Microwave Circuit Aspects of Avalanche-Diode and Transferred Electron Devices*), vol. MTT-18, pp. 808–817, Nov. 1970.
[6] M. J. Howes, "Circuit considerations in the design of wide-band tunable transferred-electron oscillators," *IEEE Trans. Electron Devices*, vol. ED-17, pp. 1060–1067, Dec. 1970.
[7] J. C. Slater, *Microwave Electronics.* New York: Van Nostrand, ch. 9, 1957.
[8] W. R. Curtice and J. J. Purcell, "Analysis of the LSA mode including effects of space charge and intervalley transfer time," *IEEE Trans. Electron Devices*, vol. ED-17, pp. 1048–1060, Dec. 1970.

On the Optimum Design of Tapered Waveguide Transitions

RUDOLF P. HECKEN AND ALFREDO ANUFF

***Abstract*—It has been found experimentally that the conventional optimization of waveguide tapers for the interconnection of circular waveguides with different diameters fails if the ratio in the diameters becomes too large. With the aid of an accurate numerical analysis program, the reason for the failure was found to be the reconversion from the unwanted mode to the main mode, which is neglected in all known synthesis procedures. The performance of tapers can be considerably improved by the implementation of other design equations and establishing new design criteria. This results in somewhat longer tapers. Various tapers were designed according to these procedures for a maximum of −40-dB H_{02}-mode level between 40 and 110 GHz, and preliminary measurements on fabricated units substantiate the improvement. It is further shown that the mode conversion at cutoff does not exhibit any singularity.**

Manuscript received August 14, 1972; revised November 31, 1972.
The authors are with Bell Laboratories, 1600 Osgood St., North Andover, Mass. 01845.

I. Introduction

INHOMOGENEOUS TEM transmission lines and waveguides in the form of tapered matching sections or tapered waveguide transitions are frequently used for very broad-band applications [1]–[3]. For the intended use of millimeter waves as a transmission medium in communication systems, tapered circular waveguide transitions are needed which do not generate spurious modes above a tolerable level [4]. The problem in the design of these inhomogeneous waveguides is basically that of specifying a distributed inhomogeneity for minimum mode conversion and/or minimum reflections over a specific frequency range. If the physical length of the device is at the same time kept at a minimum, the design is optimum.

Based on the representation of the electromagnetic field in the inhomogeneous region by an infinite set of cylindrical normal modes, an approximate analytical solution of the minimization of the mode conversion has been reported by Unger [3] and Tang [5], but it appears that these theories lack quantitative restrictions which indicate the range of validity of the approximations involved.

It has been found, experimentally at first, and then with the aid of a computer program, that the optimization of tapers based on these theories may result in large deviations from the design objectives, namely in high mode conversions. The design theory was then reexamined and the quality of the approximations checked with a digital analysis program. It turned out that all near-optimum distribution functions for the inhomogeneity fail to yield acceptable tapers, except for small differences between the waveguide radii to be interconnected by the transition.

Though the reasons for the deviations between synthesized and analyzed performance are now exactly known, it has not been possible to devise a rigorous synthesis procedure. However, the studies resulted in guidelines allowing the design of tapers which are close to an optimum design. The numerical analysis program is used to verify the performance and, if necessary, to modify the design such that the conversion does not exceed the requirements.

In the following sections, some equations forming the basis for the exact analysis and the synthesis are repeated in order to be able to point to differences between the conventional designs and to elaborate on the approximations which ultimately lead to unsatisfactory results. Although the discussion is restricted to tapered sections of circularly symmetric waveguides which are excited by H_{0n} modes only, the results and conclusions can be applied to many coupled wave problems.

II. Abstract of the Design Theory

A tapered but otherwise perfectly circular and lossless waveguide section is known schematically in Fig. 1. With an H_{01} mode incident on this inhomogeneous section, the strongest mode conversion occurs between the H_{01} and H_{02} modes. If the taper is gradual enough, the interaction with higher H_{0n} modes may be neglected, and the conversion process is described by a quadruple of coupled transmission-line equations [3]:

$$\frac{dV_n}{dz} = -j\omega\mu_0 I_n + \frac{1}{a}\frac{da}{dz}\frac{2k_n k_m}{k_m^2 - k_n^2} V_m$$

$$\frac{dI_n}{dz} = -j\frac{\beta_n^2}{\omega\mu_0} V_n + \frac{1}{a}\frac{da}{dz}\frac{2k_n k_m}{k_m^2 - k_n^2} I_m,$$

$$n = 1, m = 2, \text{ and } n = 2, m = 1. \quad (1)$$

V_n and I_n are the mode voltages and mode currents of the H_{0n} mode. $\beta_n(z)$ is the propagation constant of the nth mode propagating in a cylindrical waveguide of a particular cross section having a radius $a(z)$:

$$\beta_n^2 = \omega^2\mu_0\epsilon_0 - (k_n/a)^2$$

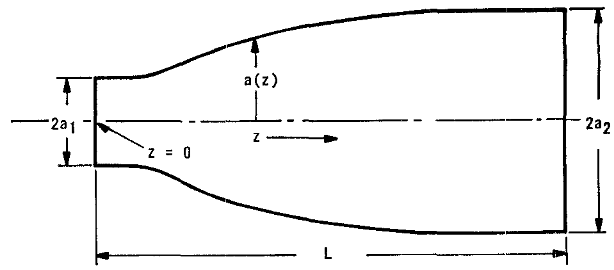

Fig. 1. Schematic view of taper contour.

where ω is the angular frequency, μ_0 the free-space magnetic permeability, ϵ_0 the permittivity of vacuum, and k_n is the nth zero of the Bessel function of the first kind, J_1. For modes above or below cutoff, Unger [3] and later Tang [5] transformed the mode voltages and currents into forward- and backward-scattered waves. However, useful design information could be obtained only after neglecting both the reflections due to the variation of the local wave impedances and the conversion into backward-scattered waves. Then (1) reduces to only a pair of coupled differential equations in forward waves of the two modes A_1 and A_2. In a further step these waves are transformed into quasi-orthogonal waves W_1 and W_2. The solution for W_2 at the end of the taper, with reconversion of W_2 into W_1 neglected, has been given as

$$|W_2(L)| \simeq \left| \int_0^{\rho_L} (2\theta) e^{-j2\rho}\, d\rho \right| \quad (2)$$

in which $\rho(z)$ can be interpreted as an accumulated phase function $[\rho_L = \rho(L)]$ while 2θ is the "distribution function" of the mode conversion along the taper.

The actual design can be accomplished with two fundamental equations:

$$\int_{a_1}^{a} q(a')\, da' = \int_0^{\rho} \sin(2\theta)\, d\rho' \quad (3)$$

and

$$z = \int_0^{\rho} \frac{\cos(2\theta)\, d\rho'}{\Delta\beta} \quad (4)$$

yielding a and z as function of ρ.

Unfortunately, these equations have been further approximated by both Unger and Tang with the result that the simplified design formulas become altogether independent of the transformation to quasi-orthogonal waves. Therefore, the contours of the tapers reported by these authors are not modified by the orthogonalization procedure. This simplification comes by replacing sin (x) and cos (x) by x and 1, respectively:

$$\int_{a_1}^{a} q(a')\, da' \cong \int_0^{\rho} (2\theta)\, d\rho' \quad (5)$$

$$z \cong \int_0^{\rho} \frac{d\rho'}{\Delta\beta}. \quad (6)$$

It should be noted that these simple design formulas could have been obtained by solving the coupled wave equations in A_1 and A_2 with reconversion from A_2 into A_1 neglected.

III. Some Experimental Results

Experimental results on a taper designed with the simplified formulas (5) and (6) are reported by Unger [3]. The $\sin^2 x$ function was chosen as the distribution function and the taper obtained is theoretically far from optimum, having a length of about 35.56 in. Mode conversion of less than 50 dB has been measured, a result supporting the approximate theory. No experimental results are reported by Tang on the optimized $\sin^3 x$ taper. However, a taper using also the optimized $\sin^3 x$ distribution in connection with the simple formula was designed elsewhere [7]. The end diameters were 0.2612 in and 2.0 in, respectively, and the maximum expected mode level was -45 dB. Measurements revealed an H_{02} level of about -25 dB. Based also on the simple design equations, another taper with end diameters of 0.375 in and 2.0 in was built for a specified mode level of -40 dB. In order to obtain shorter tapers, the modified Dolph–Chebyshev distribution function was applied [6]. Experiments with this taper indicated also a high mode level of as much as -28 dB.

IV. The Analysis of Tapered Waveguide Transitions

In order to determine exactly whether mechanical tolerances in the fabrication or other steps in the sequence of approximations cause the failure of the design, a numerical analysis program has been devised which for each desired frequency directly integrates (1) along the length z. This method, in consequence, does not suffer from the various approximations made for the purpose of obtaining a synthesis method.

The essential result of interest here is the ratio PR of the power level of mode 2 relative to the level of mode 1 at the input ($z=0$) or output ($z=L$) of the taper:

$$ML[\mathrm{dB}] = 20 \log (PR) = 20 \log \frac{\mathrm{Re}\,\{V_2 I_2^*\}}{\mathrm{Re}\,\{V_1 I_1^*\}}.$$

Fig. 2 shows the computed mode level of the tapers designed by Unger and Tang. Whereas the $\sin^2 x$ taper meets the requirement (-50-dB unwanted mode level below 75 GHz), the optimized and therefore considerably shorter design by Tang does not. Analyzing other optimized tapers with larger diameter ratios, even larger deviations were found, thus confirming the experimental results mentioned in the previous section. Obviously, the optimization yields short tapers but also an unexpectedly high unwanted mode level.

A. Tests on the Validity of the Design Equations

One of the first tests performed was to find the range of validity of the simple design equations (5) and (6) in connection with a near-optimum distribution function. In this test, tapers have been analyzed all of which were designed for 40-dB mode discrimination and the same frequency range but had different diameters at the small end while a_2 was kept constant ($a_2 = 1$ in). From Fig. 3 it is apparent that the simple design equations are only useful for tapers with a_1 larger than 0.7 in if a near-optimum distribution function is applied.

In the next test, the mode conversion of tapers has been examined which was designed on the basis of the more complicated equations (3) and (4). The distribution function and frequency range were the same as before. As it turns out (Fig. 4), a taper with a_1 even as small as 0.4 in still meets the requirement. With decreasing a_1 the deviations again become excessive, but it is interesting to note that the deviations

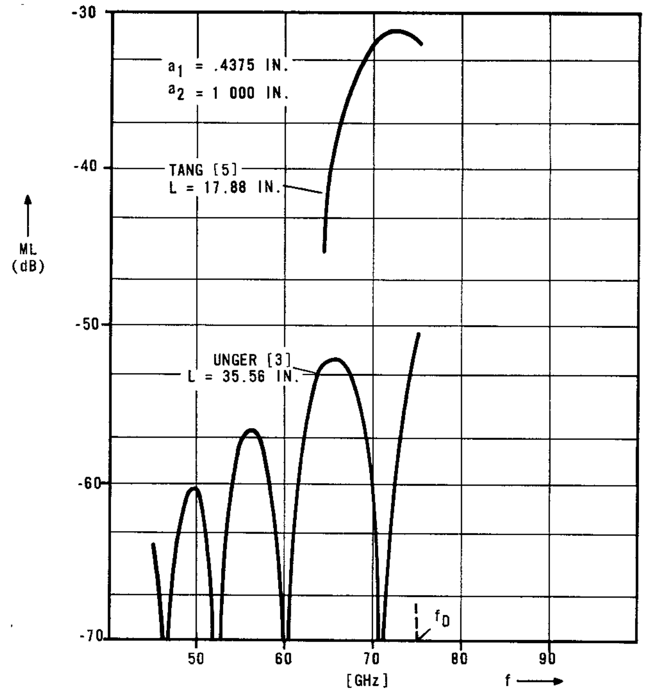

Fig. 2. Computed H_{02}-mode level of tapers designed by Unger [3] and Tang [5].

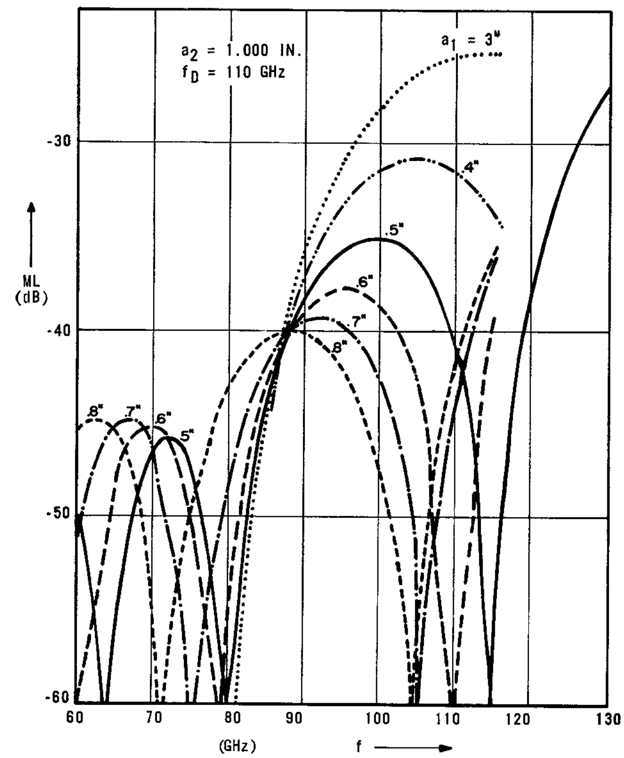

Fig. 3. *ML* as function of frequency with small end diameter as parameter [design based on (5) and (6)].

occur now at the second sidelobe. For radii larger than 0.5 in the specified mode level is never exceeded and in these cases, at least, the use of the design equations (3) and (4) must be preferred. (As an interesting case for illustration, a taper similar to Unger's example was synthesized for the same requirements, but the modified Dolph–Chebyshev distribu-

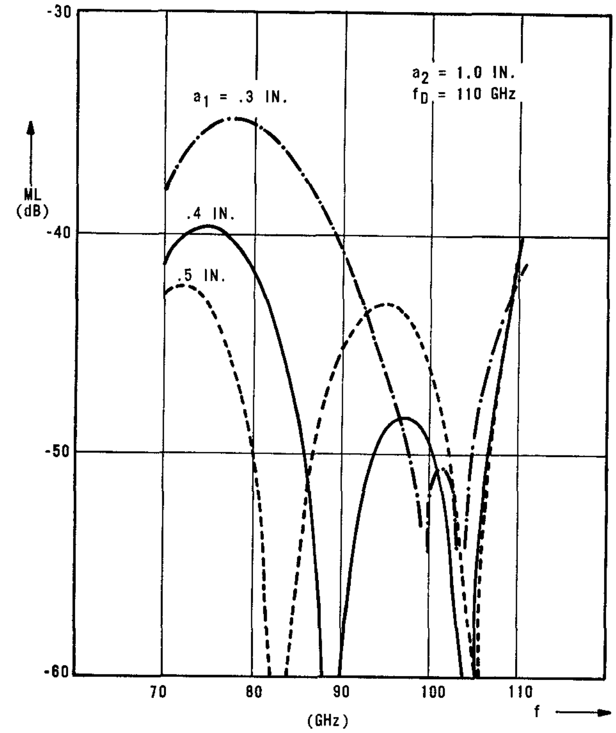

Fig. 4. ML as function of f for tapers designed with perturbation theory [(3) and (4)].

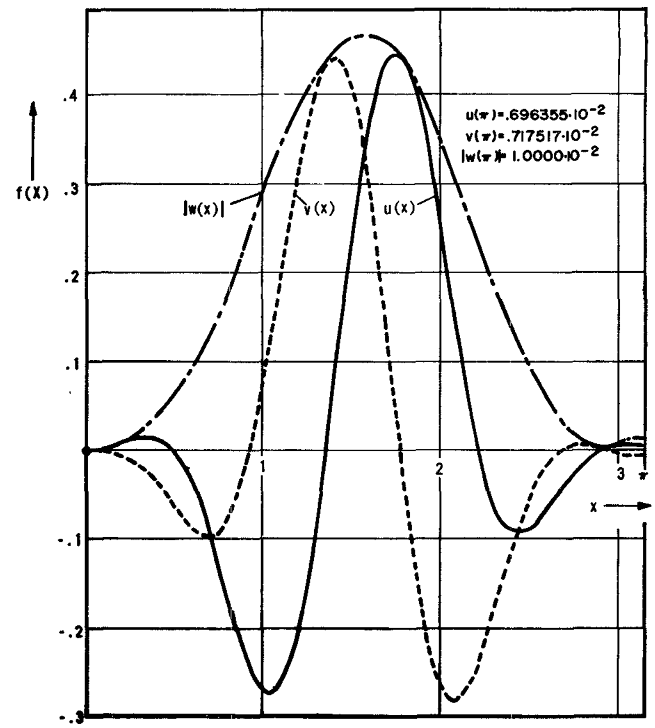

Fig. 5. $|w(x)|$, $u(x)$, and $v(x)$ for a 40-dB taper designed with the modified Dolph–Chebyshev distribution for the first sidelobe level, $\rho_1 = 7.1$.

tion and the design equations (3) and (4) were used. The analyzed mode level was -47 dB, which comes fairly close to the design goal (-50 dB). However, the length of this taper would be only 17.92 in, mainly due to the use of the modified Dolph–Chebyshev distribution.)

B. Mode Conversion Along the Taper

In the attempt to improve the design procedure for tapers with still smaller radii, another test has been performed. As is evident from the approximate solution (2), the design and the theoretical mode conversion rely on the Fourier integral:

$$w(x) = u(x) + jv(x) = \int_0^x (2\theta) e^{-j(2\rho_L/\pi)x'} \, dx' \qquad (7)$$

where a new variable has been introduced with $x = \pi(\rho/\rho_L)$. Using for 2θ the modified Dolph–Chebyshev distribution of a 40-dB taper ($a_1 = 0.1875$ in; $a_2 = 1.0$ in) and for ρ_L its minimum value $\rho_{L\,\min}$, (7) has been numerically integrated for values of x between 0 and π. Fig. 5 depicts $|w(x)|$ which builds up to a large maximum at $x = \pi/2$ along the taper, and decreases thereafter to its "correct" value at $x = \pi$. This large value of $|w(x)|$ at the center of the distribution indicates that within a certain region the coupling from mode 2 to mode 1, i.e., reconversion, might not be negligible in an optimized design.

To prove this, the analysis program has been modified so as to eliminate the reconversion in (1). This condition still maintains the effects of reflections of both waves *and* the coupling from mode 1 into both the forward- and the backwards-traveling waves of mode 2. Analyzing the failing 40-dB taper with this modified program showed that the taper under these artificial conditions would have exactly the specified mode conversion, a result which establishes the following two important conclusions. 1) Since the design equations do not account for the reflections and coupling to backward modes, these effects are in fact still negligible. 2) In the conventional optimized design of tapers with large ratios of a_2/a_1, it is the reconversion from mode 2 to mode 1 which causes large deviations from the objectives.

V. An Improved Design Procedure

Knowing the essential error in the synthesis, one has two obvious means at hand to improve the design theory such that any optimum or near-optimum distribution function is meaningful.

A. Iterative Solution

One possibility is to use the wave equations without any further approximations and to derive the design information from a more accurate iterative solution. The resulting procedure is complicated and yields tapers whose analyzed performance meets (as it should) exactly the specified requirement at the design frequency if a sufficient number of iterations is made. However, below the design frequency the performance is still poor if $a_1 < 0.4$ in. Thus this attempt is not useful.

B. Design with Larger Values for $\rho_{L\,\min}$

The other and more effective method to design short but satisfactory tapers relies on the possibility of forcing the approximate solution (2) to be valid, even when applying a (near-) optimum distribution. This is done by increasing ρ_L beyond its "minimum" value. In view of (7), this corresponds to an increase of the oscillations (see Fig. 5) of the real and imaginary parts of $w(x)$ and, as a consequence, it entails more frequent cancellations in the functions $u(x)$ and $v(x)$, thus preventing the rapid buildup of their amplitudes to extreme values. The true minimum for ρ_L must, in general, be determined for each design by trial and error, which may become cumbersome as the following brief description shows.

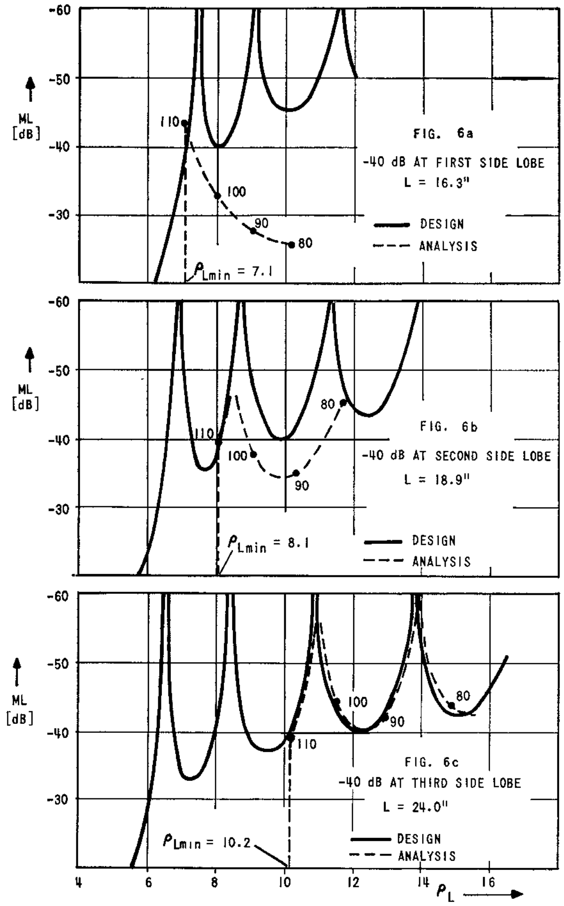

Fig. 6. Theoretical and computed mode level as function of the accumulated phase ρ_L for three different tapers designed with modified Dolph–Chebyshev distribution.

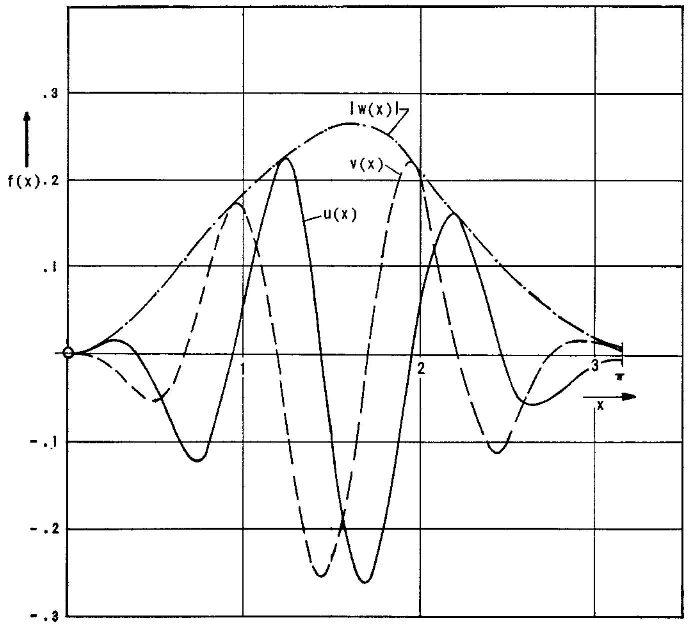

Fig. 7. $|w(x)|$, $u(x)$, and $v(x)$ for a 40-dB taper designed for the third sidelobe level, $\rho_3 = 10.2$.

The procedure can be based either on the simple design equations (5) and (6) or on the more accurate equations (3) and (4). In the following example we will use the latter because they lead to slightly (≈ 5 percent) shorter tapers.

Fig. 6 shows three different graphs of the response of the modified Dolph–Chebyshev distribution, each corresponding to three different ripple parameters B [6]. Their values have been chosen such that either the maximum of the first, second, or third sidelobe reach the desired mode level of -40 dB. For each B value one finds a value $\rho_{L\,\min}$.[1] For these three pairs of parameters (B and $\rho_{L\,\min}$), tapers have been synthesized and subsequently analyzed in Fig. 6. The design for the first sidelobe level ($\rho_1 = 7.1$) deviates by 13.4 dB, but this taper is only 16.3 in long. The design for the second sidelobe ($\rho_2 = 8.1$) is still in error by as much as 6 dB, whereas the design for the third sidelobe ($\rho_3 = 10.2$) shows an error of only 0.1 dB at the highest frequency. The lengths of these two tapers are 18.9 in and 24.0 in, respectively.

C. Mode Conversion Along a Taper of the Improved Design

It is instructive to examine again the function $w(x)$ for the case where $\rho_{L\,\min} = \rho_3 = 10.2$. From Fig. 7 one finds, surprisingly, that the maximum mode level along the taper is not much smaller than in the case of the conventional design for the first sidelobe level. However, the amplitude of mode 2 (represented by $|w(x)|$) builds up more gently and remains at a relatively high level over a wide range of x.

From these observations we come to the conclusion that the approximate solution of the coupled wave equations must be mainly in error due to the continuous phase distortion of the main mode caused by the spurious mode. This, however, produces a large phase error in the spurious mode itself which then, of course, does not behave in the way implied by the Fourier integral-type solution (7).

D. Modification of Design Equation (6)

The sensitivity of a design on phase distortions is shown by the following experiment. Recognizing that (5) specifies the increments of the magnitude of mode 2 and that (6) determines the right amount of phase of that particular increment, the latter has been arbitrarily modified into

$$z = \int_0^{\rho} \frac{d\rho'}{\Delta\beta[(1 - \epsilon(\rho')]}$$

where $\epsilon(\rho)$ is an empirical function of the type

$$\epsilon(\rho) = W_\epsilon \sin(\pi\rho/\rho_L)$$

with W_ϵ being a small value found by experimentation. Using this equation together with the corresponding equation (6), various tapers having a -40-dB mode level at the second sidelobe ($\rho_2 = 8.1$) have been synthesized and analyzed. Fig. 8 shows the response of an example with $W_\epsilon = 0.05$. This taper meets the requirement over the whole frequency range and is only 20.68 in long.

VI. Experimental Results on a Design with Phase Distortion

Based on the analysis of the last design example (Fig. 8), several tapers have been built. Since reliable measurements of spurious modes at levels below -40 dB are extremely difficult and require elaborate equipment, the following simple test

[1] The smallest value $\rho_{L\,\min} = \rho_1$ corresponds to the first sidelobe and is the one used in the conventional design method.

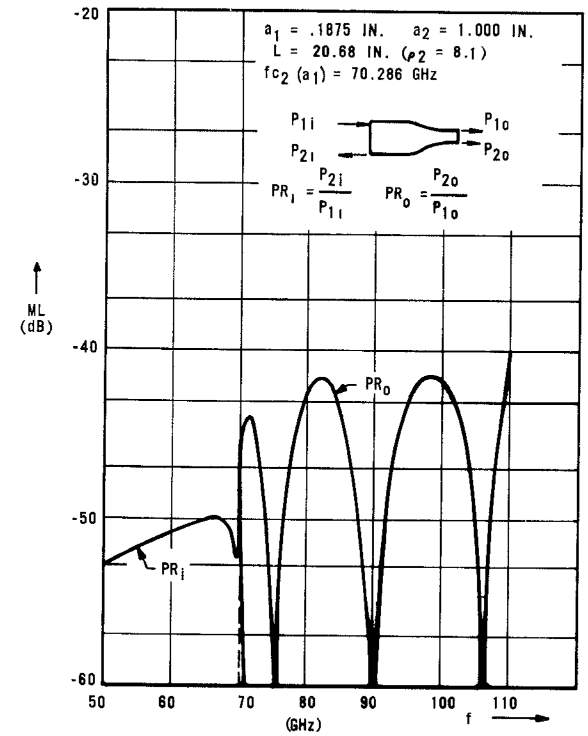

Fig. 8. Computed mode conversion of a taper designed with phase predistortion (experimental model).

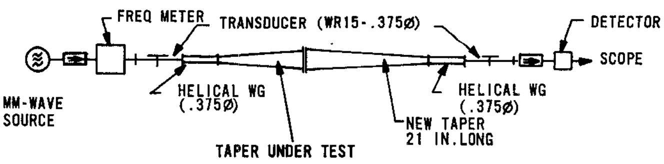

Fig. 9. Circuit to detect spurious modes.

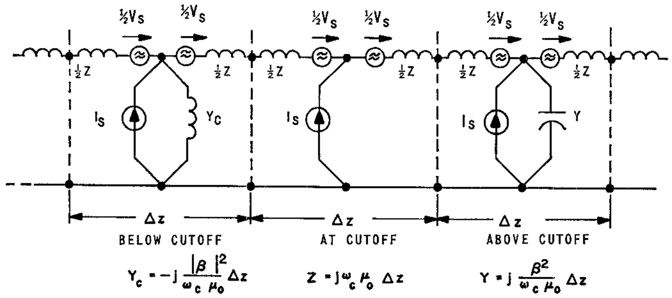

Fig. 10. Equivalent circuit of tapered waveguide section in the vicinity of a cross section at cutoff.

was performed. By mounting two tapers back to back as shown in Fig. 9, a resonant cavity for H_{02} modes is obtained for frequencies below the lowest cutoff frequency f_{c2} which is determined by the smallest radius a_1. By transmitting an H_{01} mode with $f<f_{c2}$ through this two-port, the H_{02} mode generated inside is trapped in the cavity and causes a sharp increase in the insertion loss of the H_{01} mode at discrete frequencies [8]. A resonance spike of less than 0.1 dB was the largest in amplitude which could be identified between 60 and 70 GHz. Below 60 GHz, no resonance spikes were detectable. In a similar experiment, one of the new tapers was replaced by one of the earlier designs. In this case, spikes of about 12 dB occur which may be compared with the 0.1 dB of the first experiment.

Taking the analyzed mode level (−28 dB at 69 GHz) and using [8, fig. 3], the 12-dB resonance spikes correspond to cavity losses of about 0.01 dB for the H_{02} mode. Scaling up these losses to 0.02 dB because of the increase in length of the new taper, the spike of 0.1 dB corresponds to −50 dB, comparing favorably with the analysis (Fig. 8). Even if one assumes losses of 0.1 dB in the new taper the spike of 0.1 dB corresponds to a maximum mode level of −42 dB. This gives us a strong indication that the actual performance should be close to the expectations.

VII. The Mode Conversion Below and at Cutoff

The experiment mentioned before and the analysis of various other tapers showed that the mode conversion at cutoff does not exhibit a singularity as implied in [9][2] and continues to decrease at frequencies below cutoff. This can easily be explained with the aid of an equivalent lumped-element circuit derived from (1) for the H_{02} mode.

Fig. 10 shows a few sections neighboring the cross section at cutoff. V_S, I_S represent the voltage and current sources impressed by the H_{01} mode through mode conversion. To the left and away from this cross section, the H_{02}-mode voltage and mode current are strongly attenuated when transmitted to either left or right. The cutoff section itself differs from the others in that the admittance per unit length $j(\beta^2/\omega\mu_0)$ vanishes. The voltages V_S and currents I_S, though, remain finite and excite an H_{02} wave with small amplitude, propagating to the right and becoming part of the accumulated mode 2 in the propagating section of the taper. The transmission to the left is, of course, strongly attenuated through reflection by the sections below cutoff.

For further illustration, an amplified and cutout view of Fig. 8 is presented in Fig. 11. The computation of the mode conversion was performed with the H_{01} mode incident at the large end diameter. Above cutoff, the H_{02} mode appears with significant energy at the small end only. When the frequency decreases and crosses the cutoff frequency, the output power P_{20} decreases rapidly but monotonic to zero. However, the energy of the H_{02} mode at the input increases to about the level which was observed at the output above cutoff. Below the cutoff frequency, all energy converted into the H_{02} mode between the input and the cutoff region is reflected and must appear at the input.

VIII. Conclusions

It has been shown that the conventional optimized taper designs fails if the ratio of the end diameter becomes too large. The reason for this was found to be the fact that the reconversion from the spurious mode to the incident mode is neglected. By implementing well-known but complicated design equations, the design can be considerably improved. A further improvement is possible if the design is based on the specification of the second or third sidelobe level as design objective and/or applying phase predistortion. From a pure synthesis point of view this solution is hardly attractive and a genuine optimization remains desirable. However, as long as there is no exact and explicit solution of the coupled-wave

[2] Incidentally, the calculations in [9] are in error below and also closely above cutoff due to use of wrong initial boundary conditions at $z=0$.

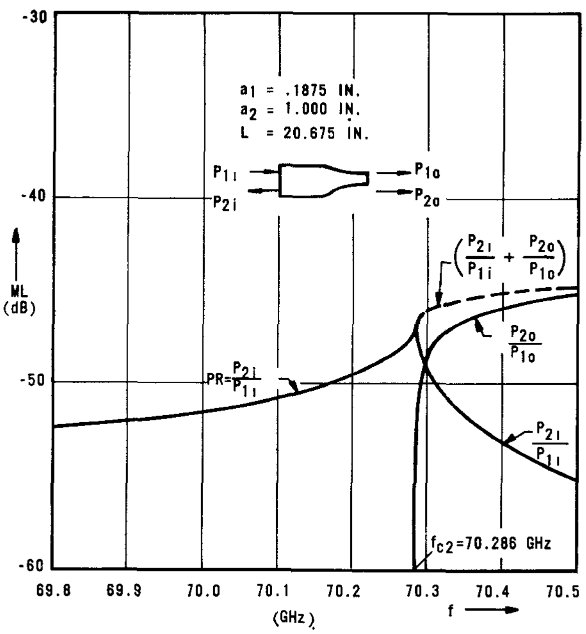

Fig. 11. Computed mode conversion of the 40-dB taper in the vicinity of the cutoff frequency of the H_{02} mode.

equations available, such an optimization has to be performed numerically. This is no trivial problem because of the severe constraint that, at least for manufacturing reasons, the slope should be continuous and monotonic. Nevertheless, with available computer programs for synthesis and analysis combined, the design of tapers for any mode discrimination and ratios a_2/a_1 can be accomplished in a short time if an interactive operating mode is possible.

Designed with this method, various 40-dB tapers having a small end diameter of 0.375 in and a large end diameter of 2.0 in were built. The H_{02} level found in a preliminary test agrees with the computed results and is below -40 dB. Moreover, it has been found that the mode conversion at cutoff of the spurious mode does not show any anomalies.

Acknowledgment

The authors wish to thank T. A. Abele, M. L. Liou, and H. C. Wang for their continuous support, as well as G. M. Blair and T. Kuliopulos for their efforts in manufacturing and finishing the tapers.

References

[1] R. W. Klopfenstein, "A transmission line taper of improved design," *Proc. IRE*, vol. 44, pp. 31–35, Jan. 1956.
[2] R. E. Collin, "The optimum tapered transmission line matching section," *Proc. IRE*, vol. 44, pp. 539–548, Apr. 1956.
[3] H. G. Unger, "Circular waveguide taper of improved design," *Bell Syst. Tech. J.*, vol. 37, pp. 899–912, 1958.
[4] S. E. Miller, "Waveguide as a communication medium," *Bell Syst. Tech. J.*, vol. 33, pp. 1209–1265, 1954.
[5] C. C. H. Tang, "Optimization of waveguide tapers capable of multimode propagation," *IRE Trans. Microwave Theory and Tech.*, vol. MTT-9, pp. 442–452, Sept. 1961.
[6] R. P. Hecken, "A near optimum matching section without discontinuities," *IEEE Trans. Microwave Theory and Tech.*, vol. MTT-20, pp. 734–739, Nov. 1972.
[7] M. A. Gerdine, Bell Laboratories, private communication.
[8] E. A. Marcatili and A. P. King, "Transmission loss due to resonance of loosely-coupled modes in a multi-mode system," *Bell Syst. Tech. J.*, vol. 35, pp. 899–906, 1956.
[9] C. C. H. Tang, "Forward and backward scattered modes in multimode nonuniform transitions," *IEEE Trans. Microwave Theory and Tech.*, vol. MTT-16, pp. 494–502, Aug. 1968.

Calculation of Inductance of Finite-Length Strips and its Variation with Frequency

A. GOPINATH AND P. SILVESTER

***Abstract*—The inductances of finite-length strips over a ground plane are calculated by the Galerkin method. The formulation is in terms of the quasi-static skin-effect equation. The numerical technique used is discussed and sample results are presented.**

Manuscript received August 18, 1972; revised January 21, 1972. This work was supported by the Communications Research Centre, Ottawa, and by the National Research Council of Canada. This work was performed while A. Gopinath was a Visiting Research Fellow at McGill University.

A. Gopinath was with McGill University, Montreal, Que., Canada. He is now with the School of Electronic Engineering Science, University College of North Wales, Bangor, Caerns, United Kingdom.
P. Silvester is with the Department of Electrical Engineering, McGill University, Montreal, Que., Canada.

I. Introduction

THE CALCULATION of inductance of finite-length conducting strips is currently of some interest. The strips concerned, for example, could take the form of interconnections between active and passive elements in integrated circuits or alternatively guiding structures such as microstrip lines in microwave integrated-circuit modules. In general, semiempirical formulas of Grover [1] are used, but these are not always satisfactory, nor are they comprehensive.

The capacitances associated with such structures have been calculated by several authors [2]–[4] and use, among